

ChemComm

Accepted Manuscript



This is an *Accepted Manuscript*, which has been through the Royal Society of Chemistry peer review process and has been accepted for publication.

Accepted Manuscripts are published online shortly after acceptance, before technical editing, formatting and proof reading. Using this free service, authors can make their results available to the community, in citable form, before we publish the edited article. We will replace this *Accepted Manuscript* with the edited and formatted *Advance Article* as soon as it is available.

You can find more information about *Accepted Manuscripts* in the [Information for Authors](#).

Please note that technical editing may introduce minor changes to the text and/or graphics, which may alter content. The journal's standard [Terms & Conditions](#) and the [Ethical guidelines](#) still apply. In no event shall the Royal Society of Chemistry be held responsible for any errors or omissions in this *Accepted Manuscript* or any consequences arising from the use of any information it contains.



ChemComm

COMMUNICATION

Intensified π -hole in beryllium-doped boron nitride meshes: its determinant role in CO₂ conversion into hydrocarbon fuel†

Received 00th September 2015
Accepted 00th XXXX 2016

Luis Miguel Azofra,^a Douglas R. MacFarlane^a and Chenghua Sun*^a

DOI: 10.1039/c5cc00000x

www.rsc.org/chemcomm

DFT investigations on beryllium-doped boron nitride meshes or sheets (BNs) predict the existence of a very reactive kind of novel material capable to spontaneously reduce the first hydrogenation step in the CO₂ conversion mechanism. This impressive behaviour appears as result of the very deep π -hole generated by the beryllium moieties, and also determines its selectivity towards the production of CH₄.

Based on data provided by NOAA,¹ the concentration of atmospheric carbon dioxide (CO₂) is increasing at the rate of 2 ppm/year.² The massive anthropogenic emissions of CO₂ into the environment highlight our heavy reliance on fossil fuels: an energy source compromising progress with the intensified greenhouse effect³ ↓ a serious environmental problem directly related with climate change.⁴ Attending to that, the search of alternatives for the diminution of CO₂ emissions deserves priority attention.⁵

Thereby, CO₂ conversion technology has as its goal the generation of 'green fuels' from CO₂ that can be re-burned for energy generation with a zero-balance of greenhouse emissions.⁶ Focusing on a (photo)-electrochemical strategy,⁷ two main aspects of the mechanism are very significant. On the one hand, CO₂ reduction requires an interaction with the catalytic surface that is usually non-spontaneous at room temperature. On the other, the first reduction step, represented by CO₂ + e⁻ → CO₂•⁻, demands a considerable input of energy⁸ and constitutes a strong limiting step in the catalytic process. Although researchers have addressed these challenges through novel chemisorption strategies⁹ and the use of semiconductors to 'artificially mimic' plant based photosynthesis mechanisms using sunlight,¹⁰ the challenge lies into finding of novel and better approaches to address these severe obstacles. Finally, depending on the number of H⁺/e⁻ pairs transferred in the overall electrochemical process, different

products such as CO, HCOOH, H₂CO, CH₃OH, or CH₄ can be obtained. In this regard, the nature of the surface material strongly affects the selectivity towards the formation of one product against another.

The analysis of the molecular electrostatic potential (MEP) on the 0.001 a.u. scale electron density iso-surface can provide clear information about the location of electron-rich and poor zones and allows a quantitative evaluation of their minima and maxima.¹¹ These points represent candidate-binding sites with complementary electron-poor and rich groups from partner molecules, and the deeper are their electrostatic potential values, the stronger the interactions that can be expected.¹²

While minima are usually associated with entities such as lone pairs, aromatic π electrons, or negatively charged moieties, maxima represent positive holes, which can be of σ or π nature depending on whether they are along or perpendicular to the direction of the bond axis, respectively. In the case at hand, electropositive atoms constituting 2D materials lead to the presence of π -holes that can potentially attach to O lone pairs of CO₂ or the radical C•/O• moieties that are produced as intermediate species in the reduction process.

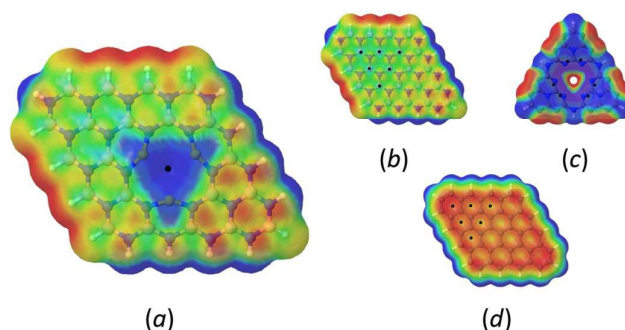


Fig. 1. MEP (± 0.02 a.u.) on the 0.001 a.u. electron density iso-surface for: (a) Be-doped BN; (b) pure BN; (c) g-C₃N₄; and (d) graphene quantum dots. Representative π -holes are indicated as black spheres on the iso-surfaces.

^a ARC Centre of Excellence for Electromaterials Science (ACES), School of Chemistry, Faculty of Science, Monash University, Clayton, VIC 3800, Australia. Tel: (+61) 3 9902 9916; Fax: (+61) 3 9905 4597; E-mail: Chenghua.Sun@monash.edu

† Electronic Supplementary Information (ESI) available: Computational details, structures and energies. See DOI: 10.1039/c5cc00000x

COMMUNICATION

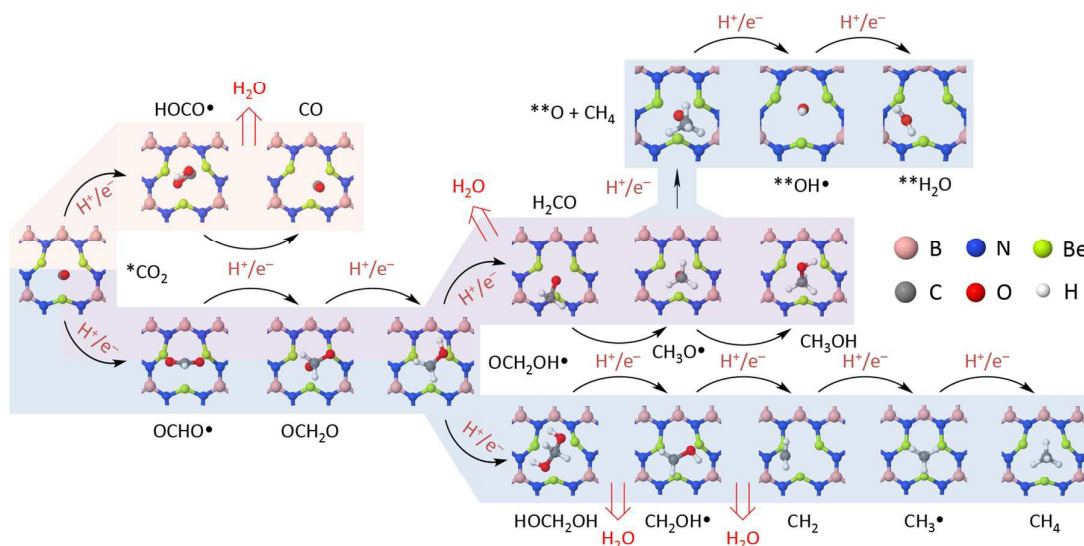


Fig. 2. Structures of the reaction sites for minimum energy paths from CO_2 to CO , CH_3OH , or CH_4 (light red, lilac and blue, respectively).

Boron nitride nano-meshes or sheets (BNs) are graphene-like 2D materials that exhibit interesting properties.¹³ Recent investigations indicate that pure BNs have the ability to produce CO_2 chemisorption once an extra electron is injected into the material, in a spontaneous process without activation barrier that can also occur by effect of an external electric field.¹⁴ Thus the goal of the present work is to demonstrate whether 2D BNs can exhibit deep π -holes when doped with electron deficient atoms such as beryllium. Our hypothesis is that this would reinforce the electrostatic interactions between the surface and CO_2 or the intermediate species in the reduction process, and therefore, dramatically decrease the energy required for the first H^+/e^- transfer, classically, the limiting step of the whole reaction. In this sense, our DFT findings open a new perspective on the computationally based design of CO_2 reduction catalysts and will hopefully stimulate further development of beryllium-based novel materials and their applications in green fuels generation technology.

Among the many BNs modifications by non-metal doping that have studied in this work by DFT computational methods [pnictogen (P, As), tetrel (C, Si, and Ge), chalcogen (O, S, and Se) and other Be-based substitutions have been performed; full details in Fig. S1 at the Electronic Supplementary Information, ESI], beryllium doping appeared to be the most promising in respect of the catalytic reduction of CO_2 . As indicated in Fig. 1, where three beryllium atoms have been

substituted for boron in the pure BN quantum dot, generate a very deep π -hole being $V_{s,\text{max}} \approx 3.6$ eV. As result of this, the interaction of the Be-doped mesh with CO_2 leads to a physisorbed state through a set of beryllium bonds¹⁵ with a spontaneous binding Gibbs free energy at room temperature equal to -0.45 eV and interatomic $\text{R}(\text{O} \cdots \text{Be})$ distances between 2.2 and 2.3 Å. For comparative purposes, *g*- C_3N_4 exhibits lower values being $V_{s,\text{max}} \approx 1.7$ eV, while the shallow of these maxima in pure BN (≈ 0.3 - 0.4 eV) or even the negative values in graphene (as local maxima surrounded by negative electrostatic potentials) indicate poor interactions between CO_2 and these materials, however and as happens in most of the materials, it is predicted that H_2O adsorption is competitive vs. CO_2 fixation for Be-doped BNs. In any case, our results suggest that there is a direct relationship between the deep of π -holes and the energy required for the CO_2 :surface interactions, which we hypothesise to be directly related to the catalytic role at this stage (see Fig. S2).

Pure BNs as well as most of the common materials used in this process show non-spontaneous ΔG^{298} values. More significant effects become manifest in the subsequent hydrogenation steps. As shown in Fig. 2, the beryllium environment acts as catalytic site producing CO_2 conversion into CO , CH_3OH , or CH_4 compounds. The mechanism indicates the existence of two main reaction paths, dependent on where the first H^+/e^- pair transfer occurs. On the one hand, the

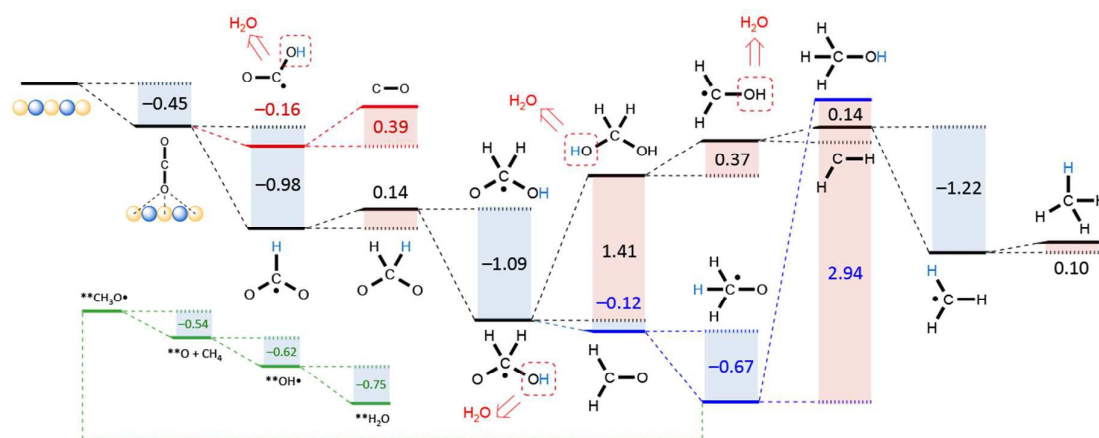


Fig. 3. Energy diagram (relative reaction Gibbs free energies at 298.15 K are shown in eV) for the reduction of CO_2 into CO (red), CH_3OH (blue), and CH_4 compounds, catalysed by Be-doped BNs. Two alternative paths (black and green) can be described for CH_4 production; the black path leading to release of H_2O prior to CH_4 , and the green path *vice versa*.

hydrogenation of the O atom of CO_2 that is not interacting with the mesh leads to the formation of the HOCO^\bullet intermediate species. This is a precursor to carbon monoxide (CO) since addition of another H^+/e^- pair on the previously hydrogenated O atom produces the release of one H_2O molecule. On the other hand, if the first hydrogenation/reduction step takes place at the C atom of CO_2 , the OCHO^\bullet radical appears as a precursor to methanol (CH_3OH) and methane (CH_4) in the subsequent fifth and seventh H^+/e^- pair electrochemical additions, respectively. It is noteworthy that both HOCO^\bullet and OCHO^\bullet radicals can merge into a common species if the second H^+/e^- pair transfer occurs on the alternate site, i.e. the addition of H^+/e^- on the C atom of HOCO^\bullet or on the O atom of OCHO^\bullet , leading to the formation of formic acid (HCOOH). Nonetheless and contrary to what is observed for pure BNs (see Fig. S3 at ESI), Be-doped BNs are non-selective towards the production of HCOOH .

Thus, unravelling the minimum energy path followed by the OCHO^\bullet radical the further, second and third gain of H^+/e^- pairs, were performed on the previously hydrogenated C and the non-interacting O atoms, leading to the OCH_2O and $\text{OCH}_2\text{OH}^\bullet$ intermediate species. This critical step is the splitting of the path into two sub-paths, since if the fourth H^+/e^- pair transfer occurs on the OH moiety in $\text{OCH}_2\text{OH}^\bullet$, it results in the formation of formaldehyde (H_2CO) with the release of one H_2O molecule to finally reach CH_3OH , however if it takes place on the O atom interacting with the mesh, methanediol [$\text{CH}_2(\text{OH})_2$]

is obtained and CH_4 is the final hydrocarbon product in four subsequent H^+/e^- gains.

Concerning the path towards the formation of CH_3OH , the internal C=O distance in H_2CO is actually elongated to 1.52 Å. The very strong interaction of the O moiety with two berylliums causes the strengthening of the two $\text{Be}\cdots\text{O}$ bonds with interatomic distances of 1.64 and 1.70 Å and the complementary distortion of H_2CO . This behaviour is also present in the OCH_2O second-order reduced intermediate species as well as in the $\text{OCH}_2\text{OH}^\bullet$ radical.

The analysis of the energy diagram corresponding to the minimum energy path (see complementary information in Fig. S4 at ESI) summarised in Fig. 3 for the reduction of CO_2 into CO, CH_3OH , or CH_4 indicates that, both the HOCO^\bullet and OCHO^\bullet radicals created as result of the first H^+/e^- pair transfer, exhibit spontaneous reaction Gibbs free energies at 298.15 K (hereafter referred simply as reaction energy), amounting to -0.16 and -0.98 eV, respectively. It is often thought that the first step demands a considerable input of energy,⁸ and often constitutes the limiting step of the whole process. In this regard, the very negative and therefore spontaneous energy values obtained by us are in sharp contrast with such hypotheses, and open a promising direction based on beryllium-doped materials. Undoubtedly, the high stability of the HOCO^\bullet and OCHO^\bullet intermediate species is also explained by their strong interactions with the mesh *via* the reinforced π -hole generated. For instance, OCHO^\bullet exhibits two symmetric $\text{O}\cdots\text{Be}$ bonds with very close interatomic distances of 1.60 Å.

By comparison, our calculation for the first H^+/e^- pair gain to reach $OCHO\bullet$ catalysed by pure BNs displays a reaction barrier around 2.4 eV, suggesting that these materials are not efficient catalysts for the reduction of CO_2 in agreement with the very poor π -holes displayed in such meshes (Fig. S3).

Both the formaldehyde and methanediol pathways to reach, in each case, methanol and methane, share a common path up to the third hydrogenation step. The second H^+/e^- pair transfer is performed on the C atom of the $OCHO\bullet$ radical requiring the injection of 0.14 eV. Furthermore, the OCH_2O intermediate species is spontaneously reduced to $OCH_2OH\bullet$ with a release of 1.09 eV. Despite the distorted H_2CO as well as the $CH_3O\bullet$ intermediate species are spontaneously formed with reaction energies of -0.12 and -0.67 eV, respectively, a huge reaction barrier of 2.94 eV is required for the final formation of the CH_3OH fuel. Why? Obviously, the entry of the sixth H^+/e^- to the $CH_3O\bullet$ radical requires its release, however the very strong interaction between this and the mesh through three $O\cdots Be$ bonds with interatomic distances equal to 1.65 Å discourages this catalytic path. In such sense, it seems quite evident that the O-philicity of the beryllium network system plays a determining role in the capture of molecules containing carbonyl or non-hydrogenated O motifs, so that for the release of these molecules an important amount of energy is required. Notwithstanding, and as has been proposed by Peterson *et al.*,¹⁶ an alternative path from the $CH_3O\bullet$ radical (green in Fig. 3), involving first the production of CH_4 and second the production of H_2O by reduction of the O atom contaminating the mesh, occurs as a cascade of spontaneous processes.

In the case of the methanediol path for CH_4 production (black path in Fig. 3), its pathway reveals that $OCH_2OH\bullet$ is reduced including the fourth H^+/e^- pair on the interacting with the mesh O atom to reach $CH_2(OH)_2$. As happens in the previous case, the $OCH_2OH\bullet$ needs to be released from the sheet to enhance its reaction with H^+/e^- . This process also demands the injection of energy, however this certainly limiting step only requires 1.41 eV. Finally, this methanediol pathway indicates that the successive fifth and sixth hydrogenations produce the release of two H_2O molecules, with small reaction energies of 0.37 and 0.14 eV, in each case. The elimination of the O atoms from the substrate prevents the appearance of a huge reaction barrier such as reported for the $CH_3O\bullet/CH_3OH$ case and leads to methylene (CH_2) that weaker interacts with the mesh forming an angularly stressed three-membered Be–C–N ring. As result of the O elimination *via* the formation of two released H_2O molecules, the seventh and last H^+/e^- pair transfers finally produce $CH_3\bullet$ and CH_4 , being the first a spontaneous process with the release of energy in 1.22 eV, and the second one, only demanding 0.10 eV. However, the alternative involving first the CH_4 production and second the H_2O release along the sixth and eighth steps seems to be thermodynamically preferred.

In summary, the very deep π -hole exhibited by Be-doped BNs produces a very reactive kind of material capable of strongly catalysing the first hydrogenation step of CO_2 reduction. Impressively, spontaneous reaction energies of $-$

0.16 and -0.98 eV are achieved for the production of the $HOCO\bullet$ and $OCHO\bullet$ radical species, respectively.

For comparative purposes, theoretical calculations using copper-based materials as catalysts show non-spontaneous values of ≈ 0.4 eV for the $CO_2/HOCO\bullet$ step.^{6c,16} This highlights the determinant role that plays the intensified π -hole generated by the beryllium moieties, opening a promising direction in the development of novel beryllium-based materials. This work also demonstrates that computational tools can be very useful in the design of CO_2 catalysts.

Authors acknowledge the Australian Research Council (ARC) for its support through ACES, Discover Project (DP130100268, CS), Future Fellowship (FT130100076, CS), and Laureate Fellow (DRM) schemes. The National Computational Infrastructure (NCI) is also acknowledged for providing the computational resources.

Notes and references

- National Oceanic and Atmospheric Administration (NOAA) Earth System Research Laboratory. <http://www.noaa.gov>
- E. J. Maginn, *J. Phys. Chem. Lett.*, 2010, **1**, 3478.
- T. R. Karl and K. E. Trenberth, *Science*, 2003, **302**, 1719.
- (a) R. A. Betts, O. Boucher, M. Collins, P. M. Cox, P. D. Falloon, N. Gedney, D. L. Hemming, C. Huntingford, C. D. Jones, D. M. H. Sexton and M. J. Webb, *Nature*, 2007, **448**, 1037; (b) J. Meyer, *Nature*, 2008, **455**, 733.
- D. T. Whipple and P. J. A. Kenis, *J. Phys. Chem. Lett.*, 2010, **1**, 3451.
- (a) C. W. Li and M. W. Kanan, *J. Am. Chem. Soc.*, 2012, **134**, 7231; (b) L. Liu, H. Zhao, J. M. Andino and Y. Li, *ACS Catal.*, 2012, **2**, 1817; (c) J. Graciani, K. Mudiyansele, F. Xu, A. E. Baber, J. Evans, S. D. Senanayake, D. J. Stacchiola, P. Liu, J. Hrbek, J. F. Sanz and J. A. Rodriguez, *Science*, 2014, **345**, 546; (d) X. Min and M. W. Kanan, *J. Am. Chem. Soc.*, 2015, **137**, 4701.
- S. N. Habisreutinger, L. Schmidt-Mende and J. K. Stolarczyk, *Angew. Chem. Int. Ed.*, 2013, **52**, 7372.
- W. H. Koppenol and J. D. Rush, *J. Phys. Chem.*, 1987, **91**, 4429.
- X. Meng, S. Ouyang, T. Kako, P. Li, Q. Yu, T. Wang and J. Ye, *Chem. Commun.*, 2014, **50**, 11517.
- H. Li, X. Zhang and D. R. MacFarlane, *Adv. Energy Mater.*, 2015, **5**, 1401077.
- J. S. Murray and P. Politzer, *WIREs Comput. Mol. Sci.*, 2011, **1**, 153.
- L. M. Azofra, I. Alkorta and S. Scheiner, *Phys. Chem. Chem. Phys.*, 2014, **16**, 18974.
- (a) R. T. Paine and C. K. Narula, *Chem. Rev.*, 1990, **90**, 73; (b) D. Golberg, Y. Bando, Y. Huang, T. Terao, M. Mitome, C. Tang and C. Zhi, *ACS Nano*, 2010, **4**, 2979; (c) H. Choi, Y. C. Park, Y.-H. Kim and Y. S. Lee, *J. Am. Chem. Soc.*, 2011, **133**, 2084.
- (a) Q. Sun, Z. Li, D. J. Searles, Y. Chen, G. Lu and A. Du, *J. Am. Chem. Soc.*, 2013, **135**, 8246; (b) H. Guo, W. Zhang, N. Lu, Z. Zhuo, X. C. Zeng, X. Wu and J. Yang, *J. Phys. Chem. C*, 2015, **119**, 6912.
- M. Yáñez, P. Sanz, O. Mó, I. Alkorta and J. Elguero, *J. Chem. Theory Comput.*, 2009, **5**, 2763.
- A. A. Peterson, F. Abild-Pedersen, F. Studt, J. Rossmeisl and J. K. Nørskov, *Energy Environ. Sci.*, 2010, **3**, 1311.